# Type 2 $Cu^{2+}$ in pMMO from *Methylomicrobium album* BG8

Hua Yuan,* Mary Lynne Perille Collins,# and William E. Antholine*
*Biophysics Institute, Medical College of Wisconsin, Milwaukee, Wisconsin 53226, and #Department of Biological Sciences and Great Lakes Water Institute, The University of Wisconsin-Milwaukee, Milwaukee, Wisconsin 53201 USA

ABSTRACT EPR spectra were obtained for the type 2 $Cu^{2+}$ site in particulate methane monooxygenase (pMMO) from *Methylomicrobium album* BG8 grown on $K^{15}NO_3$ and $^{63}Cu(NO_3)_2$. The concentration of the type 2 $Cu^{2+}$ signal was ~200 $\mu$M per 25 mg/ml protein in packed cells and membrane fractions, a concentration that is consistent with its attribution to pMMO, and the EPR parameters were consistent with electron paramagnetic resonance (EPR) parameters previously assigned to pMMO. The superhyperfine structure due to nitrogen is better resolved because $I = 1/2$ for $^{15}N$ whereas $I = 1$ for $^{14}N$ and $A(^{15}N)/A(^{14}N) = 1.4$. Under these conditions, superhyperfine structure is resolved in the $g_{\|}$ region of the X-band spectrum. At low microwave frequency (S-band) the resolution of the nitrogen superhyperfine structure improves. Signals are attributed to type 2 $Cu^{2+}$ in which cupric ion is bound to four (less likely three) nitrogen donor atoms.

## INTRODUCTION

Methane monooxygenases (MMOs) are enzymes that convert methane to methanol (Hanson et al., 1991; Hanson and Hanson, 1996; Anthony, 1986).

$$CH_4 + O_2 + NAD(P)H + H^+ \rightleftharpoons CH_3OH + H_2O + NAD(P)^+$$

Distinct soluble (sMMO) and particulate (pMMO) enzymes occur. Much is known about the oxo-bridged dinuclear iron center in sMMO (Rosenzweig et al., 1993; Lipscomb, 1994), but much less is known about the copper center(s) in pMMO. Whereas pMMO is present in all known methanotrophic bacteria, sMMO is limited to some strains and is made only under conditions of copper limitation (Prior and Dalton, 1985). The pMMO from *Methylococcus capsulatus* (Bath) consists of three subunits of 47, 27, and 25 kDa. Electron spin paramagnetic resonance (EPR)-detectable $Cu^{2+}$ from pMMO in cells has been correlated to activity (Nguyen et al., 1994, 1996; Chan et al., 1993). Chan, Lidstrom, and co-workers have proposed a mechanism for dioxygen reduction and methane activation by a trinuclear copper cluster (Chan et al., 1993). Recently, mechanistic hypotheses (Elliott et al., 1997) for dioxygen adducts based on a dicopper-oxo core, as described in model complexes (Halfen et al., 1996; Mahapatra et al., 1996), included three schemes involving direct insertion of an activated oxygen atom into the pro-(R) C-H bond or a concerted pairwise process or hydrogen atom abstraction followed by attack of an oxygen-based radical. Regardless of the mechanism, alkane hydroxylation proceeds favoring attack at the C-2 position (Elliott et al., 1997). DiSpirito and co-workers have presented an alternative model in which the catalytic site involves both iron and copper, although they reserve the option of a single ferrous iron center or an iron-iron center (Zahn and DiSpirito, 1996).

The source of pMMO for many of the studies is *M. capsulatus* (Bath), which is capable of making both pMMO and sMMO. In this work, the source of pMMO is *Methylomicrobium album* BG8, in which only copper-loaded pMMO is present. Analysis of pMMO from an organism incapable of making sMMO is advantageous because it has been suggested that under some circumstances sMMO can co-purify with pMMO (Nguyen et al., 1998). It is possible that the differences reported in studies of pMMO from *M. capsulatus* (Bath) are attributable to sMMO. In our previous EPR study of signals from *M. album* BG8 (Yuan et al., 1997), we concluded that the cupric EPR signal obtained as isolated or upon reduction of pMMO is not a signal from a mixed valence delocalized copper trimer as previously described by others (Nguyen et al., 1994). Either three or four nitrogen donor atoms contribute to the nitrogen superhyperfine pattern on the $M_I = -1/2$ line in the $g_{\|}$ region, but it was too difficult to distinguish between a seven-line pattern with relative intensities of 1:3:6:7:6:3:1 for three approximately equivalent nitrogens and a nine-line pattern with relative intensities of 1:4:10:16:19:16:10:4:1 for four equivalent nitrogens, especially when the outer lines with intensity of 1 are buried in the noise. The data reported here are consistent with four nitrogens bound in a square planar configuration from analysis of whole cells grown on a $^{15}N$ isotope. Whole cells are used for this analysis to preserve the environment around the copper.

One of the intriguing aspects of copper in pMMO is the report of the large number of coppers per pMMO consisting of the 47-, 27-, and 25-kDa subunits (Nguyen et al., 1994, 1996, 1998; Chan et al., 1993; Zahn et al., 1996). The inferred amino acid sequence is known for the three subunits (Murrell and Holmes, 1996; Semrau et al., 1995), but

*Received for publication 6 July 1998 and in final form 18 January 1999.*

Address reprint requests to Dr. William E. Antholine, Biophysics Research Institute, Medical College of Wisconsin, 8701 Watertown Plank Road, Milwaukee, WI 53226. Tel.: 414-456-4032; Fax: 414-456-6512; E-mail: wantholi@mcw.edu.

H. Yuan's current address: The Scripps Research Institute, 10550 North Torrey Pines Road, La Jolla, CA 92037.



0006-3495/99/04/2223/07 $2.00

as yet, no copper-binding sites have been identified. The Chan model proposes 15–21 Cu atoms arranged in E-clusters for the electron transfer sites and C clusters for the catalytic sites grouped into seven trinuclear copper clusters (Nguyen et al., 1994, 1996; Chan et al., 1993). Approximately 70% to 80% of the copper ions exist as Cu(1+) in the "as isolated" form as determined by x-ray absorption (Nguyen et al., 1994, 1996; Chan et al., 1993). The pMMO preparation isolated by Zahn and DiSpirito (1996) contains 2.5 iron atoms and 14.5 copper atoms per 99 kDa from three major polypeptides with molecular masses of 47, 27, and 25 kDa. The EPR spectrum of the enzyme is attributed to a type 2 copper center ($g_z = 2.057$, $g_\parallel = 2.24$, and $A_\parallel = 174$ G), a weak high-spin iron signal ($g = 6$), and a broad low-field signal ($g = 12.5$).

This study focuses on the EPR-detectable type 2 $Cu^{2+}$ from pMMO in cells of *M. album* BG8. The type 2 $Cu^{2+}$ site is further characterized using EPR methods on *M. album* BG8 cells grown on $K^{15}NO_3$. Finally, a model in which type 2 $Cu^{2+}$ is bound to the amino-terminal histidine, is discussed.

## MATERIALS AND METHODS

### Growth of bacterium

*M. album* BG8 was grown in the batch culture in nitrate mineral salts (NMS) medium (Whittenbury et al., 1970) containing 5 $\mu$M cupric sulfate. Cultures were incubated at 30°C with shaking at 150 rpm in a 50% methane, 50% air (v/v) atmosphere. After growth for 2 days, cells were harvested by centrifugation at 8000 rpm for 30 min at 4°C. The cell pellets were washed twice in ice-cold 20 mM phosphate, 5 mM magnesium chloride buffer (pH 7.0) and collected at 10,000 rpm for 10 min. For isotope studies, cells were grown in the same medium by the same process except potassium nitrate was replaced by $^{15}N$-potassium nitrate (Aldrich, Milwaukee, WI) and cupric sulfate replaced by 63-cupric nitrate (Cambridge Isotope Laboratories, Andover, MA).

### Enzyme activity

MMO activity was detected by propylene oxidation by whole cells. Cells grown with sufficient copper to saturate the growth requirements in the medium (Collins et al., 1991; Brantner et al., 1997) had an optimal MMO activity under our conditions of 21 nmol/min/mg protein.

### Peptide synthesis

A 20-amino-acid peptide, HGEKSQAAFMRMRTIHWYDL, was synthesized by solid-state methods on an automated Milligen Biosearch peptide synthesizer (model 9050) at the Protein/Nucleic Acid Shared Facility at the Medical College of Wisconsin. After synthesis, the peptide was reduced by dithiothreitol and purified by high-pressure liquid chromatography. The purified peptide was then stored in sealed test tubes purged with argon.

A stock solution was prepared by dissolving 1.2 mg of peptide in 150 $\mu$l of 0.1% trifluoroacetic acid (TFA) in double-distilled water. A series of samples was prepared by adding $^{63}Cu(NO_3)_2$ to the peptide according to the molar ratio of copper to peptide. Samples with ratios of $Cu^{2+}$ to peptide of 1:1,1:2, 1:3, and 1:4 were diluted by HEPES buffer (pH 7.2), and the pH was adjusted before freezing the sample in liquid nitrogen.

### EPR measurements

All X-band spectra were recorded on a Varian E109 Century Series spectrometer with a Varian TE102 cavity (Varian, Palo Alto, CA). Samples were placed in a finger dewar filled with liquid nitrogen. The concentration of $Cu^{2+}$ in the sample was calculated by comparing the double integral of the spectrum with the double integral of the spectrum from a 1.0 mM cupric perchlorate solution. S-band (3.4 GHz) spectra were obtained from a spectrometer with a loop-gap resonator cavity and a low-frequency microwave bridge built at the National Biomedical ESR Center, Medical College of Wisconsin. S-band samples were cooled by nitrogen passed through an exchange coil immersed in liquid nitrogen. Microwave frequencies were measured with a frequency counter (EIP model 548), and the field was calibrated with a magnetometer (Rawson-Lush Instrument Co., Acton, MA). Spectra were simulated using a program from Lynn Belford (University of Illinois, Urbana, IL) (Nigles, 1979; Maurice, 1980).

## RESULTS AND DISCUSSION

### X-band (9.2 GHz) EPR spectroscopy

EPR spectra from whole cells of *M. album* BG8 grown on both $^{63}Cu^{2+}$ and $K^{15}NO_3$ are better resolved than spectra from whole cells grown on $^{63}Cu$ and $K^{14}NO_3$ (Fig. 1 and

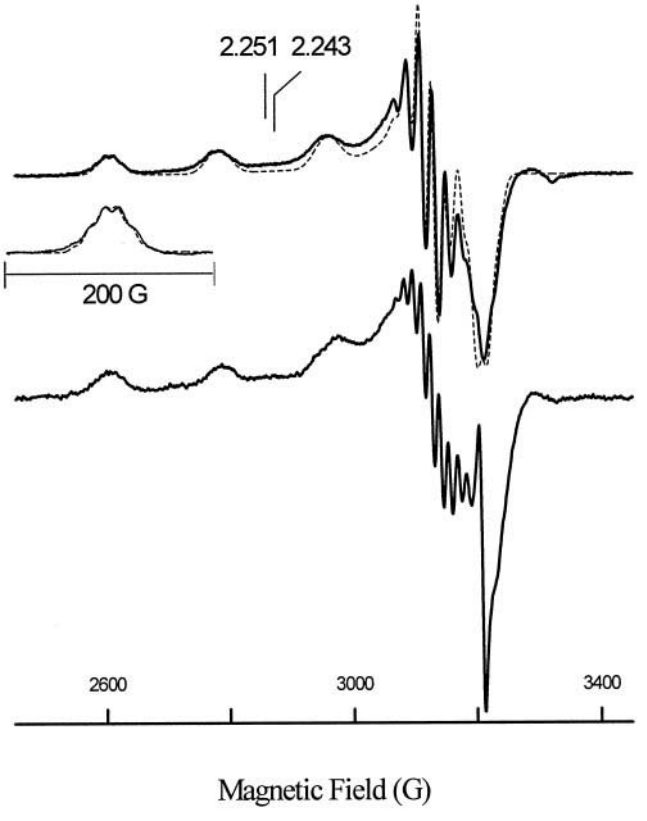


FIGURE 1 X-band EPR spectra (*upper trace*) of *M. album* BG8 cells grown with $^{15}N$ and $^{63}Cu^{2+}$. The upper spectrum is the average of four scans. The insert is the expansion of the $-3/2$ line in the $g_\parallel$ region after 15 scans. The dotted lines are simulations. Spectrometer conditions: microwave frequency, 9.089 GHz; modulation amplitude, 5 G; microwave power, 5 mW; temperature, 77 K. Simulated spectra are the sum of two spectra, A and B. Simulation parameters are listed in Table 1. Spectrum B: same parameters as used for spectrum A except $g_z = 2.251$. X-band EPR spectrum (*lower trace*) of *M. album* BG8 cells grown with $^{14}N$ and $^{63}Cu^{2+}$.

Yuan et al., 1997). As the nitrogens bound to the type 2 $Cu^{2+}$ are $^{15}N$ instead of $^{14}N$, the superhyperfine pattern changes because $I = 1/2$ for $^{15}N$ and $I = 1$ for $^{14}N$. Also, the spectra are better resolved because $A(^{15}N)/A(^{14}N) = 1.4$. Specifically, the $M_I = -3/2$ line and to a lesser extent the $M_I = -1/2$ line in the $g_\parallel$ region are split into multiple lines not resolved in previous spectra with $^{14}N$ donor atoms. Also, there are fewer, better resolved lines in the $g_z$ region. As the pattern is dependent on microwave frequency (see S-band spectrum discussed later), the better resolved lines on the $M_I = -3/2$ line in the $g_\parallel$ region are attributed to the superposition of two spectra with $g_\parallel = 2.243$ and 2.251, respectively, and with the same $A_\parallel^{Cu}$ value of 180 G (Fig. 1). The coupling (180 G) taken for $A_\parallel$ from the difference in field between the $M_I = -3/2$ and $-1/2$ copper lines is less than the parameter for $A_\parallel$ used in the simulations because of second-order shifts. Given that the $M_I = -3/2$ line is the superposition of two lines, a superhyperfine coupling of ~18 G is apparent (see expanded region, Fig. 1). This coupling is consistent with the previously obtained coupling of 13 G for $^{14}N$ (Yuan et al., 1997). Six lines are resolved on the $M_I = -3/2$ line in the $g_\parallel$ region. These lines appear to originate from multi-line patterns from two superimposed lines. Five-line patterns are consistent with four $^{15}N$ ligands bound to $Cu^{2+}$ in each of two very similar complexes.

The lines in the $g_\perp$ region are split by 20 G. In previously published spectra (Yuan et al., 1997), the lines in the $g_\perp$ region were split by 14 G. Thus, these lines can be assigned to $^{15}N$ and $^{14}N$ couplings, respectively. Consistent with this argument is that the number of lines are reduced in the $g_\perp$ region with samples with $^{15}N$ donor atoms in comparison with samples with $^{14}N$ donor atoms. Twenty lines ($5 \times 4$) are expected for four equivalent $^{15}N$ donor atoms, and 36 lines ($9 \times 4$) are expected for four equivalent $^{14}N$ donor atoms plus lines for the overshoot peak and forbidden transitions. Of these lines, only approximately nine lines in the $g_\perp$ region are resolved for the sample with $^{15}N$, so many of the lines are superimposed.

## S-band (3.4 GHz) EPR spectroscopy

S-band spectra from whole cells of *M. album* BG8 grown on $^{63}Cu$ and $K^{15}NO_3$ have well resolved superhyperfine structure in the $g_\parallel$ and $g_\perp$ regions (Fig. 2). Two experimental spectra are shown in Fig. 2, one with an intense free radical signal and one with little free radical signal. Spectra with and without the free radical are obtained routinely, but the source of the free radical is not known. At room temperature the radical signal is immobilized; i.e., it has $g_\perp = 2.035$ and $g_\parallel = 2.008$ (spectrum not shown), which implies that the molecular weight of the radical complex is large and most likely from a protein. The hyperfine lines in the $g_\parallel$ region from both complexes of $Cu^{2+}$, as determined from the X-band spectrum, are superimposed at low microwave frequencies. The five-line pattern on the $M_I = -1/2$ line in the $g_\parallel$ region (Fig. 2, expanded region) is attributed to four

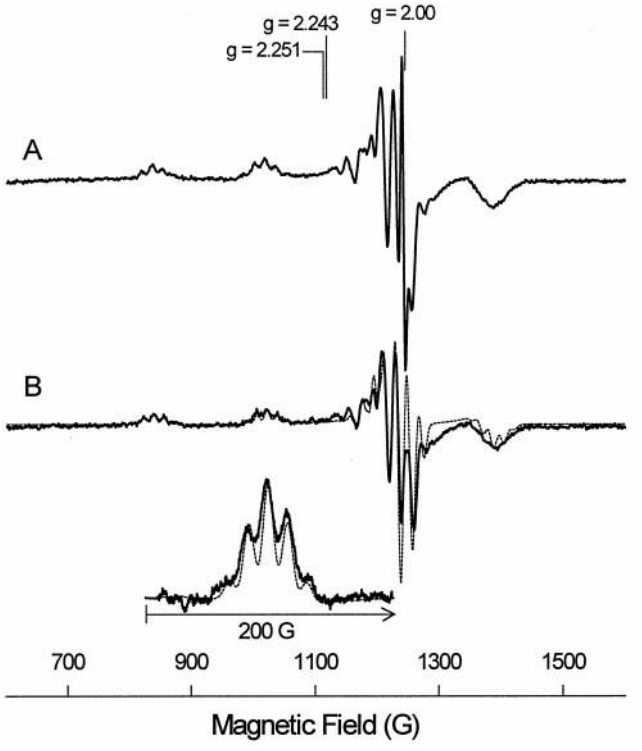


FIGURE 2 S-band EPR spectra of *M. album* BG8 cells grown with $^{15}N$ and $^{63}Cu^{2+}$. (*A* and *B*) Spectra with and without free radical, respectively. (*Inset*) The expansion of the $-1/2$ line in the $g_\parallel$ region of the S-band spectrum averaged by 30 scans. The dotted lines are simulated spectra. Spectrometer conditions: microwave frequency, 3.455 GHz; modulation amplitude, 5 G; microwave power, 22 dB; incident power, 10 mW; temperature, 140°C. Simulated are the sum of two spectra with simulation parameters as given in Table 1, except the microwave frequency is 3.4547 GHz instead of 9.089 GHz and the Euler angle $\beta$ is 2° instead of 0°.

approximately equivalent nitrogen donor atoms, each with $I = 1/2$. Previously, the signal-to-noise for the $M_I = -1/2$ line from cells grown on a $^{14}N$ source was insufficient to distinguish between three and four nitrogen donor atoms (Yuan et al., 1997). The signal-to-noise for spectra from cells grown on $^{15}N$ is sufficient to resolve a five-line pattern with relative intensities of 1:4:6:4:1 and assign four nitrogen donor atoms to $Cu^{2+}$ as compared with a four-line pattern with relative intensities of 1:3:3:1 from three nitrogen donor atoms, if the two $g_\parallel$ values are separated by ~18 G.

## Simulations

The dashed lines in Figs. 1 and 2 are simulations of the type 2 $Cu^{2+}$ at X-band and S-band frequencies using the same EPR parameters except for the microwave frequency. An iterative procedure is used, first simulating the X-band spectrum, then using these parameters for the initial values for the S-band spectrum, improving the fit of the experimental and simulated spectrum at S-band, and using these parameters to fit the X-band spectrum. For this study, two X-band spectra with $g_\parallel = 2.243$ and $g_\parallel = 2.251$, respectively, are simulated and added together. Then two S-band

spectra with $g_{\|} = 2.243$ and $g_{\|} = 2.251$ are simulated and added together (Table 1).

The number of lines and the positions of the lines are well matched between the experimental and the simulated spectra. The intensities of the simulated lines and the line widths of the experimental and simulated spectra are very similar but are not completely matched, especially in the $g_{\perp}$ region. There are three line-width parameters to fit: residual line widths (*Wx*, *Wy*, and *Wz*), *g*-strain ($C_{1X}$, $C_{1Y}$, and $C_{1Z}$), and *A*-strain ($C_{2X}$, $C_{2Y}$, and $C_{2Z}$) plus Euler angles and quadrupole terms. As there are three resolved $Cu^{2+}$ lines in the $g_{\|}$ region at two frequencies, 9.1 and 3.4 GHz, the number of variables is overdetermined. The fits are consistent with the experimental spectra but may not be unique fits. If the *g* and *A* axes are not coincident, Euler angles describe the relative orientations of these axes. A $\beta$ angle of 2° is used in the fits of the S-band spectra to increase the relative intensity of the $g_{\|}$ region with respect to the $g_{\perp}$ region. This $\beta$ angle rotates a tensor about the *x* axis, displacing the *z* axis for the A-tensor 2° from the axial direction. Although rotation of $\beta$ improves the fit, other parameter changes that also may increase the intensity of $g_{\|}$ with respect to $g_{\perp}$ lines have not been tried.

The simulations show that the two resolved patterns in the $g_{\|}$ region at X-band may not be resolved at S-band, consistent with the experimental results. The simulations for the spectra with $g_{\|} = 2.243$ and $g_{\|} = 2.251$ have the same values in the $g_{\perp}$ region. These values may not be the same, but the differences between the parameters for the $g_{\perp}$ region for the two type 2 $Cu^{2+}$ complexes are most likely small and less than the differences in the $g_{\|}$ region.

A less probable possibility is that three nitrogen donor atoms that give a 1:3:3:1 pattern are bound to $Cu^{2+}$. If the second site with $^{15}N$ donor atoms is shifted ~36 G instead of 18 G at X-band frequencies (i.e., twice the superhyperfine value), two 1:3:3:1 patterns could add up to give six lines. Then at low frequency (S-band) the resulting superhyperfine pattern from $^{15}N$ would be 1:4:6:4:1. As the number of lines for the S-band pattern for type 2 $Cu^{2+}$ with $^{14}N$ is an odd number of lines (Yuan et al., 1997), four nitrogens are favored, but the argument is tentative due to the number of assumptions. In summary, the lines in the spectra from cells are attributed to signals from two very similar type 2 $Cu^{2+}$ complexes and a radical.

**TABLE 1 EPR parameters for simulations**

| | Spectrum A | Common parameters | Spectrum B |
|---|---|---|---|
| $g_z$ | 2.243 | | 2.251 |
| $g_x$, $g_y$ | | 2.059, 2.061 | |
| $A_x = A_y$, $A_z$ (MHz) | | 30, 565 | |
| $A_x^N = A_y^N$, $A_z^N$ (MHz) | | 56, 50 | |
| 2D, 2E (MHz) | | 15, 2 | |
| $W_x$, $W_y$, $W_z$ | | 10, 14 | |
| $C_{2x} = C_{2y}$, $C_{2z}$ (MHz) | | 10, 5 | |
| $C_{1x} = C_{1y}$, $C_{1z}$ (MHz) | | 1.7, −1.5 | |

To simulate the experimental data, two spectra, one with $g_z = 2.243$ and one with $g_z = 2.251$ are added together. The remaining parameters are the same for both spectra. Four equivalent nitrogens with $M_I = 1/2$ were used. $C_{2x}$, $C_{2y}$, and $C_{2z}$ are *A*-strain parameters and $C_{1x}$, $C_{1y}$, and $C_{1z}$ are *g*-strain parameters. All other parameters have the usual meaning.

## Amino acid fragment

A possible type 2 site for $Cu^{2+}$ in pMMO might involve the histidine at the amino terminal of the 47-kDa subunit. The type 2 $Cu^{2+}$ site from pMMO in cells has similar EPR parameters (Fig. 1; Table 2) to the EPR parameters for $Cu^{2+}$ GHK, the cupric complex of the tripeptide, for which $g_{\|} = 2.25$, $A_{\|} = 185$ G, and nitrogen superhyperfine structure is well resolved in the $g_{\|}$ region (data not shown). However, the histidine of the 47-kDa subunit of pMMO is the amino-terminal residue (Nguyen et al., 1994, 1996; Chan et al., 1993), not the second or third residue from the amino terminal as, for example, with GHK. Therefore, a synthetic peptide, HGEKSQAAFMRMRTIHWYDL, which mimics the amino-terminal residues of the 47-kDa subunit, was synthesized. The lines in the EPR spectrum after addition of one equivalent of $Cu^{2+}$ to one equivalent of synthetic peptide are shifted from the lines for which the ratio of $Cu^{2+}$ to peptide is 1:2 (Figure 3 *A*; Table 2) or 1:4 (data not shown). The EPR parameters from the signal for a 1:1 $Cu^{2+}$-to-peptide ratio are $g_{\|} = 2.264$ and $A_{\|} = 173$ G. EPR parameters ($g_{\|} = 2.246$, $A_{\|} = 184$ G) from the spectrum for one equivalent of $Cu^{2+}$ in the presence of two or four equivalents of synthetic peptide are closer to the EPR parameters for the type 2 $Cu^{2+}$ in pMMO. One difference is that superhyperfine structure from the nitrogen ligands is not resolved as well as the EPR-detectable site in pMMO. Nevertheless, the binding site for $Cu^{2+}$ in pMMO has characteristics of the binding of $Cu^{2+}$ to the amino terminal of a peptide with a histidine as the first amino acid. A histidine as the first amino acid provides two nitrogen donor atoms, the amine and a nitrogen in the imidazole ring. Either another bidentate amino-terminal histidine or nitrogen donor atoms from the protein, presumably from the imidazoles of histidines, are needed to provide the four nitrogen donor atoms (Fig. 4).

## Probable binding site for type 2 $Cu^{2+}$

To use the $Cu^{2+}$ EPR signal from *M. album* BG8 as a probe of the environment of the protein and the cell, a basic

**TABLE 2 EPR parameters for type 2 Cu at 77 K**

| Sample | $A_{\|}$ (G) | $g_{\|}$ | $g_{\perp}$ |
|---|---|---|---|
| *M. album* BG8 in cells | | | |
| $^{63}Cu$ (signals 1 and 2 not resolved) | 185 | 2.24 | 2.067 |
| $^{63}Cu$, $^{15}N$ signal 1 | 180 | 2.243 | 2.067 |
| $^{63}Cu$, $^{15}N$ signal 2 | 180 | 2.251 | 2.067 |
| $Cu^{2+}$-syn peptide (1:1) | 174 | 2.264 | 2.063 |
| $Cu^{2+}$-syn peptide (1:2) | 184 | 2.246 | 2.061 |
| *M. capsulatus* (Bath) (Nguyen *et al.*, 1994) | 180 | 2.25 | 2.06 |
| Cu(GHK) | 185 | 2.25 | 2.07 |

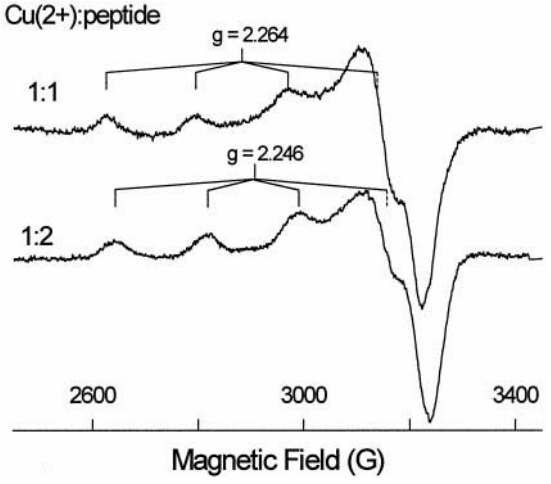


FIGURE 3 X-band EPR spectra of $Cu^{2+}$-peptide. The 20-amino-acid peptide, HGEKSQAAFMRMRTIHWYDL, was sequenced as in the amino terminus of the 47-kDa subunit. The molar ratios of $^{63}Cu^{2+}$ to peptide are shown. EPR conditions: microwave frequency, 9.105 GHz; modulation amplitude, 5 G; microwave power, 5 mW.

understanding of the EPR signal is needed. Spectra from cells and simulations (Figs. 1 and 2) provide a set of EPR parameters for square planar or pyramidyl square planar type 2 $Cu^{2+}$ complexes. The nitrogen superhyperfine structure on the lines in the $g_{\|}$ region are consistent with four approximately equivalent nitrogen donor atoms in the equatorial plane. Elliott et al. (1998) have obtained data from pulsed EPR studies of pMMO membrane samples from *Methylococcus capsulatus* (Bath) that support histidine ligation to the EPR-detectable copper. The possible existence of two type 2 Cu ions both bound to four nitrogen donor atoms was unexpected. Only signals from a type 2 Cu site formed from a single isotope of copper, $^{63}Cu$, and nitrogen donor atoms from $^{15}N$ are resolved well enough to separate the two signals. Approximately equal concentrations of both signals have been obtained in several samples from cells. Similar X-band and S-band data for the type 2 $Cu^{2+}$ site from *M. capsulatus* (Bath) are consistent with $Cu^{2+}$ bound to four nitrogen donor atoms but with only one signal with $g_{\|} = 2.251$ (unpublished results).

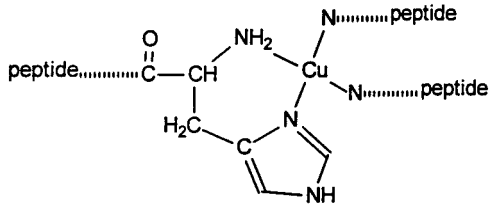


FIGURE 4 Schematic for binding of cupric ion to the amino-terminal sequence for which histidine is the first amino acid. Nitrogen donor atoms from the protein, presumably from the imidazole of histidines, provide the third and fourth nitrogen donor atoms. Alternatively, another bidentate amino-terminal histidine could complete the square planar configuration resulting in the formation of *cis* and *trans* dimers.

Much of our work on binding of $Cu^{2+}$ to proteins involves binding of $Cu^{2+}$ to the amino-terminal region, in which a histidine is either the second or third residue (Taketa and Antholine, 1982; Rakhit et al., 1985). In this study, a synthetic peptide is synthesized with a histidine as the first amino acid of the amino-terminal end. The fragment consists of the same 20 amino acids as found in the 47-kDa subunit of pMMO of *M. capsulatus* (Bath) (Zahn and DiSpirito, 1996; Murrell and Holmes, 1996; Semrau et al., 1995). Although the EPR parameters for the $Cu^{2+}$ complex of the synthetic peptide and type 2 $Cu^{2+}$ site in pMMO are well matched, the comparison is consistent with, not proof for, binding of $Cu^{2+}$ to the amino terminal of the 47-kDa subunit of pMMO. Yet the comparison is instructive. For example, when the concentration of $Cu^{2+}$ to synthetic peptide is 1:2, the configuration for $Cu^{2+}$ probably involves bidentate chelators to form a square planar complex (Fig. 4). It is anticipated that the amino-terminal end will be a good bidentate chelator for a peptide in which the first amino acid is a histidine because it is difficult to twist the first peptide amido nitrogen into the equatorial plane, whereas it is relatively easy to use a peptide amido nitrogen from the histidine for the third donor atom of a tridentate complex where histidine is the second or third amino acid. Bidentate chelation for the amino terminal of the 47-kDa subunit of pMMO also seems likely. One possible explanation for two very similar spectra for the type 2 $Cu^{2+}$ site might be a *cis* or *trans* configuration for the nitrogen donor atoms from the imidazoles of the histidines (Fig. 4). More studies need to be completed to fully understand the very similar type 2 $Cu^{2+}$ signals with $A_{\|} = 180$ G from pMMO. If the ratio of the binding of $Cu^{2+}$ to pMMO is 1:2, then the concentration of $Cu^{2+}$ from the signal with $A_{\|} = 180$ G is one-half the pMMO monomer concentration.

## Comparison of the amino-terminal amine binding site with other models

Bidentate ligation accounts for two of the four nitrogens bound as determined from the nitrogen superhyperfine structure in the low-frequency EPR spectrum. If dimers of the 47-kDa subunit exist, cupric ion could stabilize the dimer by coordinating to both bidentate amino-terminal amines and imidazoles, thus providing four approximately equivalent nitrogen donor atoms.

Others have proposed that the type 2 copper site is part of the active site in pMMOa (27 kDa) involving HIS38, HIS40, and/or HIS168, and this site may be localized at the membrane-periplasm interface (Elliott et al., 1998). If type 2 $Cu^{2+}$ does not use the amino-terminal histidine to bind $Cu^{2+}$, then this site, being a good bidentate ligand, is available to bind excess $Cu^{2+}$. Often membrane fractions contain more than one type 2 $Cu^{2+}$ EPR signal, and the extra signals could use the amino-terminal histidine for donor atoms.

There are several reasons as to why the type 2 $Cu^{2+}$ signal in *M. album* BG8 can be attributed to pMMO. First,

the concentration of the type 2 $Cu^{2+}$ is ~200 $\mu$M in BG8 cells. This concentration of the EPR-detectable cupric ion is approximately five times greater in cells with pMMO than in cells from heterotrophic bacteria that lack pMMO (Yuan et al., 1999). Also, total copper in cells with pMMO is ~10 times greater than in such cells without pMMO. Second, the EPR parameters for the type 2 $Cu^{2+}$ signal from *M. album* BG8 cells are similar to those for the signal from *M. capsulatus* (Bath) (Table 2). Finally, spectra obtained in cells are very similar to spectra obtained in membrane fractions, as expected for pMMO. Therefore, if the type 2 $Cu^{2+}$ site in pMMO from *M. capsulatus* (Bath) is part of the active site, then the type 2 $Cu^{2+}$ site in *M. album* BG8 should be part of the active site.

Analysis of the ratio of EPR-detectable type 2 cupric ion to total copper determined by atomic absorption in *M. album* BG8 suggests that there is one EPR-detectable type 2 cupric site per molecule of pMMO and two or three coppers per molecule, which are most likely $Cu^{1+}$ and not detected by EPR (Yuan et al., 1999). These numbers are more reasonable than the 15–21 coppers per molecules reported in the literature (Nguyen et al., 1994, 1996, 1998; Chan et al., 1993; Zahn et al., 1996). One can speculate as to how 15–21 coppers per molecule could be reported. One line of reasoning is that pMMO degrades upon purification and copper from degraded protein binds to intact pMMO. Some of the copper, especially with anaerobic procedures, may be $Cu^{1+}$ and not EPR detectable. For $Cu^{2+}$, the superhyperfine structure from nitrogens often is poorly resolved, which in our studies meant superposition of cupric signals. In support of this argument, it is difficult to place 3–5 coppers in sites selected from the amino acid sequence from the three subunits, much less the 15–21 coppers. The extra copper and poor resolution of the superhyperfine structure in the EPR spectra could suggest considerable pMMO degradation.

Under our conditions, no propylene-to-propylene oxide activity is found in cell extracts or membrane fractions of *M. album* BG8 cells. The results of others suggest a loss of activity during purification of pMMO from *M. capsulatus* (Bath); the purified preparation of a specific activity was only 27–41% of unfractionated membranes (Nguyen et al., 1998). Therefore, the loss of activity for our membrane fractions under aerobic conditions may not be unreasonable. Nevertheless, only studies with cells are reported in this work.

Using *M. album* BG8 cells, in our hands, no iron signals with $g = 12$ were observed. Others have suggested that signals from iron are obtained because of co-precipitation of the iron-containing sMMO with pMMO or the existence of multiple iron-containing proteins from respiratory enzymes (Nguyen et al., 1998).

In summary, ~80% of the copper in pMMO is $Cu^{1+}$ as determined from x-ray absorption (Nguyen et al., 1996). The EPR parameters for the type 2 $Cu^{2+}$ are similar in *M. capsulatus* (Bath) and *M. album* BG8. The ligands for type 2 $Cu^{2+}$ are probably four nitrogen donor atoms (three nitrogen donor atoms are possible but require many fortuitous assumptions). Histidine is bound to the EPR-detectable type 2 $Cu^{2+}$ as determined by pulsed EPR (Elliott et al., 1998). No iron is found in purified protein from *M. capsulatus* (Bath) (Nguyen et al., 1998).

There are no irrefutable EPR data for a trinuclear copper cluster. The early suggestion of 10 EPR lines from one electron distributed over three coppers was disproved by our multifrequency work (Yuan et al., 1997, 1998). We propose that the EPR signal obtained from addition of ferricyanide to pMMO is not intrinsic to pMMO but from a form of $CuFe(CN)_6^{2-}$ (Yuan et al., in press). If the addition of $Fe(CN)_6^{2-}$ gives a signal, which is not intrinsic to pMMO, there is only one report of spectroscopic data for an oxidized form of pMMO (Nguyen et al., 1994).

Although there are many similarities, especially with respect to EPR signals, between pMMO from *M. album* BG8 and *M. capsulatus* (Bath), differences have been observed. For example, the growth requirement for copper for *M. album* BG8 is 5 $\mu$M $Cu^{2+}$ (Brantner et al., 1997) whereas 20 $\mu$M $Cu^{2+}$ in the medium is typically used for *M. capsulatus* (Bath) (Semrau et al., 1995). Finally, the concentration of pMMO in *M. album* BG8 correlates with the concentration of the type 2 $Cu^{2+}$ signal; loss of activity correlates with the superposition of a second type 2 EPR signal but not with the concentration of the type 2 signal with $g_{\|} = 2.24$ and $A_{\|} = 180$ G (manuscript in preparation). Clearly, additional studies with both strains are needed, and the high resolution of the type 2 $Cu^{2+}$ signals from pMMO reported in this work should help future studies.

We thank Liane M. Mende-Mueller, Protein/Nucleic Acid Shared Facility, and Emily Marks, an intern from Alverno College, for their contribution with respect to the data from the protein fragment.

This work was supported by grant RR01008 from the National Institutes of Health and by grant MCB-9118653 from the National Science Foundation and is publication 417 from the Center for Great Lakes Studies.

## REFERENCES

Anthony, C. 1986. Bacterial oxidation of methane and methanol. *Adv. Microb. Physiol.* 27:113–209.

Brantner, C. A., L. A. Buchholz, C. C. Remsen, and M. L. P. Collins. 1997. Intracytoplasmic membrane formation in *Methylomicrobium album* BG8 is stimulated by copper in the growth medium. *Can. J. Microbiol.* 43:672–676.

Chan, S. I., H.-H. T. Nguyen, A. K. Shiemke, and M. E. Lidstrom. 1993. The copper ions in the membrane-associated methane monooxygenase. *In* Bioinorganic Chemistry of Copper. K. Karlin and Z. Tueklar, editors. Chapman and Hall, New York. 184–195.

Collins, M. L. P., L. A. Buchholz, and C. C. Remsen. 1991. Effect of copper on *Methylomonas albus* BG8. *Appl. Environ. Microbiol.* 57: 1261–1264.

Elliott, S. J., D. W. Randall, R. D. Britt, and S. I. Chan. 1998. Pulsed EPR studies of particulate methane monooxygenase from *Methylococcus capsulatus* (Bath): evidence for histidine ligation. *J. Am. Chem. Soc.* 120:3247–3248.

Elliott, S. J., M. Zhu, L. Tso, H.-H. T. Nguyen, J. H.-K. Yip, and S. I. Chan. 1997. Regio- and stereoselectivity of particulate methane monooxygenase from *Methylococcus capsulatus* (Bath). *J. Am. Chem. Soc.* 119: 9949–9955.

Halfen, J. A., S. Mahapatra, E. C. Wilkinson, S. Kaderli, V. G. Young, L. Que, A. D. Zuberbuhler, and W. B. Tolman. 1996. Reversible cleavage and formation of the dioxygen O-O bond within a dicopper complex. *Science*. 271:1397–1400.

Hanson, R. S., and T. E. Hanson. 1996. Methanotrophic bacteria. *Microbiol. Rev.* 60:439–471.

Hanson, R. S., A. I. Netrusov, and K. Tsuji. 1991. The obligate methanotrophic bacteria *Methylococcus*, *Methylomonas*, and *Methylosinus*. *In* The Procaryotes. A. Bolows, H. G. Truper, M. Dworkin, and K. Schliefer, editors. Springer Verlag, New York. 2350–2364.

Lipscomb, J. D. 1994. Biochemistry of the soluble methane monooxygenase. *Annu. Rev. Microbiol.* 48:371–399.

Mahapatra, S., J. A. Halfen, E. C. Wilkinson, G. Pan, X. Wang, V. G. Young, C. J. Cramer, L. Que, and W. B. Tolman. 1996. Structural, spectroscopic, and theoretical characterization of bis($\mu$-oxo) dicopper complexes, novel intermediates in copper-mediated dioxygen activation. *J. Am. Chem. Soc.* 118:11555–11574.

Maurice, A. M. 1980. Ph.D. thesis. University of Illinois, Urbana, IL.

Murrell, J. C., and A. J. Holmes. 1996. Molecular biology of particulate methane monooxygenase. *In* Microbial Growth on C Compounds. M. E. Lidstrom and F. R. Tabita, editors. Kluwer Academic Publishers, Amsterdam. 133–140.

Nguyen, H.-H. T., S. J. Elliott, J. H.-K. Yip, and S. I. Chan. 1998. The particulate methane monooxygenase from *Methylococcus capsulatus* (Bath) is a novel copper-containing three-subunit enzyme. *J. Biol. Chem.* 273:7957–7966.

Nguyen, H.-H. T., K. H. Nakagawa, B. Hedman, S. J. Elliott, M. E. Lidstrom, K. D. Hodgson, S. I. Chan. 1996. X-ray absorption and EPR studies on the copper ions associated with particulate methane monooxygenase from *Methylococcus capsulatus* (Bath): Cu(I) ions and their implications. *J. Am. Chem. Soc.* 118:12766–12776.

Nguyen, H.-H. T., A. K. Shiemke, L. J. Jacobs, B. J. Hales, M. E. Lidstrom, and S. I. Chan. 1994. The nature of the copper ions in the membranes containing the particulate methane monooxygenase from *Methylococcus capsulatus* (Bath). J. *Biol. Chem.* 269:14995–15005.

Nigles, M. J. 1979. Ph.D. thesis. University of Illinois, Urbana, IL.

Prior, S. D., and H. Dalton. 1985. The effect of copper ions on membrane content and methane monooxygenase activity in methanol-grown cells of *Methylococcus capsulatus* (Bath). *J. Gen. Microbiol.* 131:155–163.

Rakhit, G., W. E. Antholine, W. Froncisz, J. S. Hyde, J. R. Pilbrow, and G. R. Sinclair. 1985. Direct evidence of nitrogen coupling in copper(II) complex of bovine serum albumin by S-band electron spin resonance technique. *J. Inorg. Biochem.* 25:217–224.

Rosenzweig, A. C., C. A. Frederick, S. J. Lippard, and P. Nordlund. 1993. Crystal structure of a bacterial non-human iron hydroxylase that catalyses the biological oxidation of methane. *Nature*. 366:537–543.

Semrau, J. D., A. Chistoserdov, J. Lebron, A. Costello, J. Davagnino, E. Kenna, A. J. Holmes, R. Finch, J. C. Murrell, and M. E. Lidstrom. 1995. Particulate methane monooxygenase genes in methanotrophs. *J. Bacteriol.* 177:3071–3079.

Taketa, F., and W. E. Antholine. 1982. The oxidation of cat, human, and the cat-human hybrid hemoglobins $\alpha_2^{human}$ and $\beta_2^{cat}$ and $\alpha_2^{human}\beta_2^{cat}$ by copper (II). *J. Inorg. Biochem.* 17:109–120.

Whittenbury, R., K. C. Phillips, and J. F. Wilkinson. 1970. Enrichment, isolation, and some properties of methane-utilizing bacteria. *J. Gen. Microbiol.* 61:205–218.

Yuan, H., M. L. P. Collins, and W. E. Antholine. 1997. Low frequency EPR of the copper in particulate methane monooxygenase from *Methylomicrobium album* BG8. *J. Am. Chem. Soc.* 119:5073–5074.

Yuan, H., M. L. P. Collins, and W. E. Antholine. 1998. Analysis of type 2 Cu(2+) in pMMO from *M. album* BG8. *Biophys. J.* 74:A300.

Yuan, H., M. L. P. Collins, and W. E. Antholine. 1999. Concentration of Cu, EPR-detectable Cu, and formation of cupric-ferrocyanide in membranes with pMMO. *J. Inorg. Biochem.* In press.

Zahn, J. A., and A. A. DiSpirito. 1996. Membrane-associated methane monooxygenase from *Methylococcus capsulatus* (Bath). *J. Bacteriol.* 178:1018–1029.